BJET
(Bayero Journal of Engineering and Technology)
https://bjet.ng/index.php/jet

Research Article
2025, Vol. 20 (1), 33-43

SIMPLIFIED MODELLING AND GA-OPTIMISATION OF A PROPORTIONAL-INTEGRAL LOAD FREQUENCY CONTROLLER FOR STAND-ALONE SMALL HYDROPOWER PLANTS

M.K. Sani[1], A. Haruna[2*]

1. Department of Electrical Engineering, Bayero University, Kano - Nigeria
2. Department of Mechatronics Engineering, Bayero University, Kano - Nigeria

*Corresponding author: aharuna.mct@buk.edu.ng

Received: 31-05-2025
Revised: 24-06-2025
Accepted: 27-06-2025
Published: 04-07-2025

Abstract: *This paper presents load frequency control for standalone small hydropower plants using an electronic load controller (ELC) tuned via Genetic Algorithm (GA) optimisation. The ELC for a standalone generating system is developed using an Arduino microcontroller, solid-state relays, a zero-crossing detection circuit, and heating elements to serve as damper loads for channelling the generator's excess power during load changes using phase cut modulation. A high-fidelity (HF) MATLAB/Simulink model of the system was developed using the physical characteristics of the experimental model while a simplified transfer function model of the system with fast execution time was derived using output data obtained from the real-time experimental model and GA optimisation. GA optimisation was then used to tune a PI controller to minimise the output frequency error of the simplified model. The obtained optimised PI gains were then deployed to the HF model and the physical system in real time. Comparisons of the results by simulation and real-time experimentation show that the parameters of the phase modulated PI-controlled ELC can be tuned relatively quickly via GA optimisation with the simplified model to achieve satisfactory performance.*

Key words: Genetic algorithms, Hydropower, PI control, Phase angle control, Load frequency control.

1. Introduction

Hydropower, or hydroelectric power, is a renewable energy source that employs a dam or diversion structure to modify the natural flow of a river or other body of water. Hydropower depends on the water cycle's unending, continually replenishing mechanism to continuously harness energy. Turbines and generators are employed in hydropower to turn the kinetic energy into electricity, which is then supplied to the electrical grid to power homes and industries. hydropower is an affordable, non-polluting, and ecologically beneficial form of electricity. Significant infrastructure innovations are being implemented to increase the performance and efficiency of hydropower plants (Kishore et al., 2021), it has played an essential role in the safe, reliable, and efficient functioning of electric power networks for a long time. Hydropower not only provides energy as the largest worldwide renewable source but also bears a substantial percentage of the regulatory and balancing jobs in many power networks all over the globe (W. Yang, 2017). Hydropower plants are classified according to the size and operation they perform ranging from large hydropower with a capacity of more than 30 megawatts (MW), small hydropower plants that generate between 100 kilowatts (KW) and 10 megawatts (MW), and Micro Hydropower plants that have a capacity of up to 100 kilowatts. The small or micro units are usually installed at places close to the consumer. Hydropower plants have five major components: storage reservoir, intake tunnel, surge tank, penstock, and hydro turbine (Shahgholian, 2020). A small hydropower station is usually a run-of-river plant that consequently does not need any significant water reservoir, such as large dams (Contreras et al., 2020), (Hino & Lejeune, 2012). Only a part of the river water flow is diverted to the turbine. This makes such plants environmentally friendly.

Stand-alone hydropower plants (SHPPs), however, are generally isolated from the grid network and consequently suffer from several problems, including low storage potential and high unit costs. The major

problem associated with SHPPs, however, is keeping a constant speed value, which is directly related to the output frequency. Fluctuations in electrical demand can lead to imbalances between generation and consumption, resulting in frequency deviations, rapid changes in load, or sudden faults that can lead to transient effects on the hydropower system.

The primary objective of the controller is to minimise distortion, maintain system stability, and track the output frequency of the system to the desired reference level. Tackling these problems has led to the utilisation of electronic load controllers (ELCs) to manage the frequency and terminal voltage, even when dealing with unbalanced loads (Tyagi et al., 2022).

The ELC is, therefore, essential for regulating voltage and frequency in stand-alone hydropower systems and ensuring system stability. Researchers have utilised several feedback control algorithms for ELCs, including traditional PID controllers, intelligent controllers and enhanced controllers. These methods have demonstrated satisfactory performance in load frequency control of small hydroelectric power plants. An electronic controller can be employed to stabilise the synchronous generator of a small hydroelectric power (SHP) system by utilising resistive dump loads to absorb any excess generated electrical power. This can be achieved via the widely employed technique of phase angle control, where the firing angle of thyristors (or other power electronics devices) is used to manipulate the power absorbed by the dump loads, thereby effectively managing the output frequency of the generator. While the PI controller is relatively simple to deploy, its main drawback is that it is impacted by changes in system parameters, which leads to several problems, such as excessive ripple values and poor power and current quality. Therefore, to achieve satisfactory performance of the PID-based ELCs, the control algorithm employed has to be well-tuned either heuristically or by optimisation.

Optimisation in power systems refers to the enhancement of efficiency, reliability, and cost-effectiveness in the generation, transmission, and distribution of electrical energy. The objective is to identify optimal operating conditions while adhering to technical and operational restrictions. Some areas that require optimisation in power system operations include optimal power flow, reactive power optimisation, demand response optimisation, and economic load dispatch. The study (Mirsaeidi et al., 2023) groups optimisation techniques into three based on the history of their development, i.e., Classical Analytical-Based Method, Classical Arithmetic Programming-Based Algorithms and Modern Metaheuristic-Based Algorithms. In (C. Yang et al., 2023), optimisation is classified into two methods: mathematical optimisation, (such as Mixed Integer Linear Programming and Quadratic Programming for example) and heuristic optimisation, which includes Sunflower Optimisation (SFO), Particle Swarm Optimisation (PSO), Genetic Algorithm (GA), and others, and is discussed in (Shaheen et al., 2021). There are also optimisation techniques based on machine learning (Ruan et al., 2020), (Thirunavukkarasu et al., 2022), (Abdolrasol et al., 2021), which offer significant benefits compared to conventional methods. However, these can be quite complex and require training as they rely on artificial neural networks.

Genetic algorithm (GA) is an optimisation procedure inspired by natural selection. It is a population-based search algorithm that utilises the concept of survival of the fittest (Katoch et al., 2021). GAs are employed in several applications, like decision-making, machine learning and robotics (Lambora et al., 2019). A genetic algorithm is a heuristic algorithm that has good optimisation performance (Khan et al., 2020; Papazoglou & Biskas, 2023) as it can easily choose satisfactory solutions according to the optimisation objectives, and make up for these shortcomings by using its characteristics (Lü et al., 2020). GAs also has several applications in control systems and are frequently used to optimise feedback controllers based on a desired objective function, as exemplified in (Haruna et al., 2023). The study (Abbas & Mustafa, 2024) on a PID-controlled bioreactor showed that GA optimisation outperformed Ziegler-Nichols, Skogestad modification, and an IMC rule in terms of overshoot, disturbance rejection, and gain and phase margins. In (Metwally et al., n.d.) A PI controller improved by GA optimisation was used to solve the load frequency control problem in the electrical power system. The effectiveness of the suggested approach was evaluated in terms of the output frequency response. The suggested GA-PI method was shown to significantly improve system stability and decrease oscillation amplitude in comparison with a conventional PI controller. GA optimisation has also been used in real-time to tune an (Haruna et al., 2024) and an integral backstepping controller for a laboratory helicopter (Haruna et al., 2020). The GA based PID tuning has also been shown to be more adaptable to variations in system parameters (Ortatepe, 2023).

While GA is effective in optimising power systems, the drawback of this technique is that it can be difficult, expensive, and time-consuming to implement (Patil et al., 2024). These problems usually arise from the fact that accurate models are required

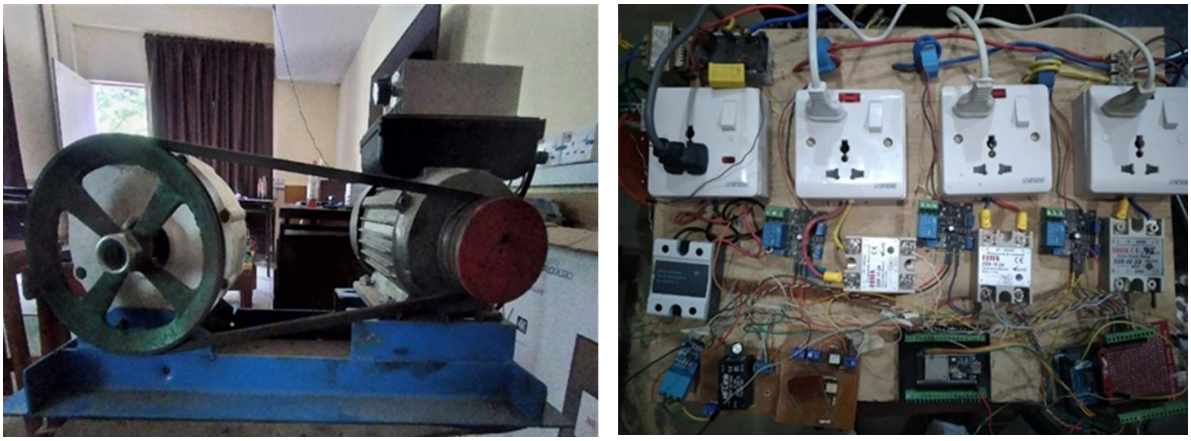

(a) (b)

Figure 1: *SHP laboratory experimental system. (a) Generating system, (b) ELC board.*

for the optimisation process, which, in the case of power systems, can be quite complex and time consuming to simulate. This paper thus proposes a GA optimized PI ELC for isolated power plants using a simplified and fast system model. A high-fidelity (HF) MATLAB/Simulink model of the physical system is first developed using the physical (electrical) characteristics of the experimental model. A simplified transfer function model of the system with fast execution time is then obtained by using GA optimisation to identify the transfer function parameters that fit output data obtained from the open-loop response of the real-time experimental model. GA optimisation is again employed to tune a PI controller to minimise the output frequency error of the simplified model. The proposed tuning approach is then validated by applying the obtained PI parameters to the HF model and real-time experimental system.

2. Materials and Methods

The experimental system, the HF model and the GA optimisation technique are discussed in this section.

2.1 Experimental setup

The system used in (Sani et al., 2024) is used for experimental validation. The model is comprised of a prime mover, 500 watts, 50 HZ, 100 V synchronous generator, resistive load, hall effect speed/rpm sensor for frequency speed measurement, MOC 3021 (Triac driven optoisolator), 4N35 optocoupler (for zero-crossing detection), solid state relays (SSRs) used for phase cutting and an Arduino Uno microcontroller. Figure 1 shows the real-time phase cut modulation experimental ELC circuitry and experimental generator set-up.

The method used in (Sani et al., 2024) was also employed to measure the real-time output frequency. A Hall rpm sensor is utilised for the frequency measurement and conversion of the three-phase synchronous generator. The generator was driven by a single-phase induction motor fed by a 220 V mains voltage supply.

The frequency of the voltage output is computed from a hall effect speed sensor placed near a magnet attached to the pulley of the generator. A pulse is generated each time the magnet completes one revolution and interacts with the hall sensor. The output of the sensor is connected to the interrupt pin (pin 2) of the Arduino Uno, so that an interrupt occurs each time the pulse changes from LOW to HIGH. The interrupt routine is programmed to measure the time between interrupts, which reflects the speed of the generator. This speed, which is directly proportional to the frequency of the voltage output, is then used to measure the frequency. To manage the power supply to the dump loads and stabilise the frequency to the nominal value of 50Hz, the phase angle is determined and chopped for each phase. The current consumed by the dump loads in each phase is measured via current transformers through the analogue pins A0, A1 and A2 of the Arduino. The pseudocode below highlights how the input from the hall sensor is converted to frequency by the Arduino.

```
function measure speed:
    set current time to current time in milliseconds
    set elapsed time to current time – last time
    IF elapsed time is greater than or equal to 1000 then:
        disable interrupt on hall sensor pin
        calculate rpm as:
            (Pulse count / 2) * 60 / (elapsed time / 1000)
        reset pulse count to 0
        enable interrupt on hall sensor pin to call count pulses on falling edge
        update last time to current time
```

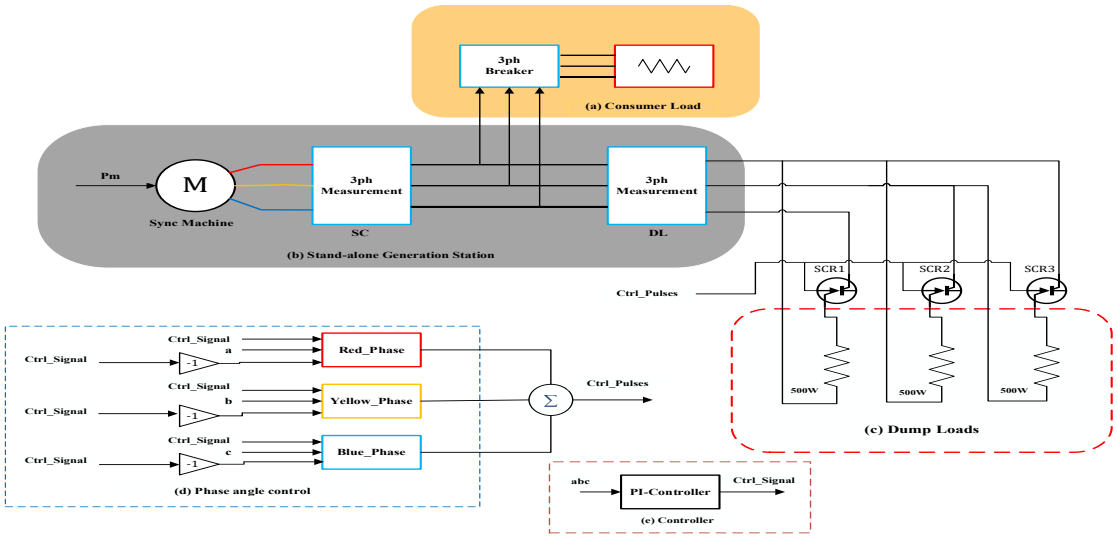

Figure 2: *PI-controlled generating system HF model. (a) Consumer load (b) Stand-alone generation station (c) Dump loads (d) Phase angle control circuitry (e) Controller*

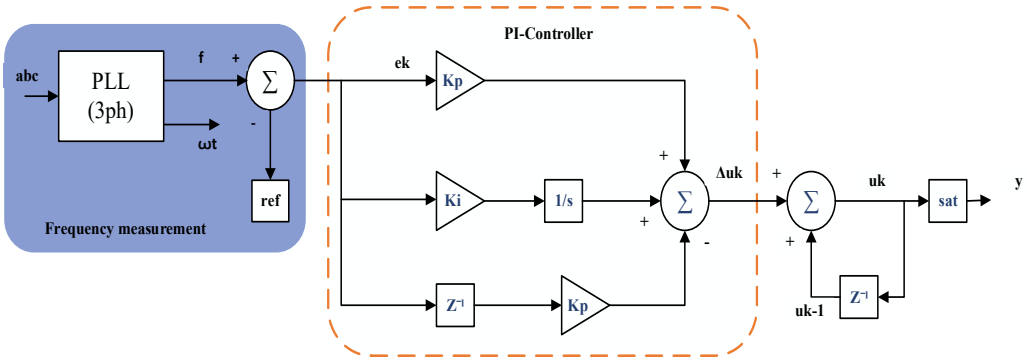

Figure 3: *PI-controlled generating system ELC*

function measure_frequency:
calculate input as (rpm * 8) / 120
return input.

Figure 2 is a block diagram of the main components of the ELC Simulink model. The ELC block is comprised of a phase lock loop (PLL), used to measure the output frequency, and a discrete PI control loop. The ELC HF Simulink model calculates the generator's output frequency and compares it with the reference frequency. In case of a deviation of the generated frequency from the reference frequency, dump loads are activated by chopping the AC sine wave (phase cut modulation) of their voltage inputs to absorb the excess energy and correct the frequency deviation. A block diagram of the system is shown in Figure 2, with the specifications of the virtual synchronous machine derived from the parameters of the experimental systems listed in Table 1. A virtual synchronous machine block with a mechanical input power is used as generating system, three-phase measurement blocks are for voltage and current measurement of the generating system and a three-phase breaker for ON and OFF automatic switching of the three-phase consumer load. The red-phase, yellow-phase and blue-phase blocks houses the phase cut circuitry for each phase; a PI-controller block provides the control signal. A detailed Simulink diagram of the HF model is shown in the Appendix for the interested reader.

Table 1: *HF Model Generator Specifications*

Specifications	Value
Active power (P)	500 W
Reactive power (Q)	500 VAR
Frequency (F)	50 Hz
Resistance (R)	0.00204 ohm
Inductance (L)	0.8104e-4 H
Inertia (J)	3.895 kgm^2

In this paper, the proportional integral (PI) controller was proposed to control the system's frequency through phase cut modulation. The controller block diagram is depicted in Figure 3 with the PI controller expressed in (1) to (4).

$$u(t) = k_p\left[e(t) + \frac{1}{T_i}\int_0^T e(t)dt\right] \quad (1)$$

$$u(t) = k_p e(t) + K_i \int_0^1 e(t)\,dt \quad (2)$$

$$\Delta u_k = \left(k_p + k_i\right)e_k - \left(k_p\right)e_{k-1} \quad (3)$$

$$u_k = u_{k-1} + \Delta u_k . [sat]_{-\pi}^{\pi} \quad (4)$$

where u_k, is the control signal, k_p and k_i respectively, are the proportional and integral gains, e_k, and e_{k-1} are the errors at the designated time steps, Δu_k is the incremental control signal and T_i is the integral time.

2.2 GA Optimisation

The functioning of GAs is closely related to two main concepts from natural evolution: natural selection and genetic dynamics, which involve various genetic operations such as crossover and mutation. The cost function assesses the performance of a candidate solution, which is the objective of the genetic algorithm to minimise or maximise. In this context, (5) and (6), respectively, are used to minimise or maximise a given cost function.

$$x = \arg\min f(x) \quad (5)$$

$$x = \arg\max f(x) \quad (6)$$

where $f(x)$ represents the cost function to be optimised, and x is the solution.

The population size refers to the count of individual candidate solutions present in each generation. The primary factor that affects diversity, convergence rate, and computational expense. A generation represents one complete cycle of evolution, where a population of candidate solutions is evaluated, selected, recombined, mutated, and replaced to form the next generation. The population is given by (7) with the fitness evaluation expressed by (8)

$$P^{(a)} = x_1^{(a)}, x_2^{(a)}, \dots \dots \dots x_p^{(a)} \quad (7)$$

$$f_n^{(a)} = f(x)_i^{(a)} \quad (8)$$

where a is the generation, P is the population size and x_n is the individual generation. Equations (9), (10) and (11) respectively give the selection, recombination (crossover) and mutation functions.

$$P_r = \left(x_n^{(a)} \text{ is selected}\right) = \frac{1}{V} . w(f_i^{(a)}) \quad (9)$$

$$x_c = \alpha x_n^{(a)} + (1-\alpha) x_i^{(a)} \quad (10)$$

$$x_c' = x_c + \delta \quad (11)$$

where $w(f)$ is the weighting function, V is the normalization factor, α is the crossover factor and x_c is a child and δ as a small random mutation. A new generation in the GA optimisation process is expressed by (12)

$$P^{(n+1)} = \text{mutate}\left(\text{crossover}\left(\text{select}\left(P^{(n)}\right)\right)\right) \quad (12)$$

In this work, the GA fitness function (13) is designed to minimise the integral of time absolute error (ITAE) for both the second-order transfer function identification and the PI-ELC tuning.

$$J_f = (\|e\|_1) / T_{sim} \quad (13)$$

where $\|e\|_1$ is the L_1 vector norm of the error and T_{sim} is the simulation time.

2.3 Simplified Model

A simplified model (SM) with a significantly faster execution time was created to emulate the HF Simulink model shown in Figure 2. The SM uses a discretised second-order transfer function, a discrete PI controller, and a consumer load modelled as a first-order discrete transfer function. The parameters of the numerator and the denominator of the generator transfer function are identified using GA to fit the open-loop output frequency response of the experimental system.

Consider the general second-order transfer function:

$$G(s) = \frac{k}{S^2 + 2\zeta\omega_n + \omega_n^2} \quad (14)$$

where ζ is the damping ratio, ω_n is the natural frequency and k is an adjustable gain. The transfer function (14) can be expressed in discrete time in the form (15)

$$G_{sm}(z) = \frac{b_0 + b_1 z^{-1}}{1 + a_1 z^{-1} + a_2 z^{-2}} \quad (15)$$

where $b_0, b_1, \in \mathbb{R}$ and $a_1, a_2 \in \mathbb{R}$, are the coefficients of the numerator and denominator respectively. A discretised transfer function is used to allow for simulation using a fixed time interval equivalent to the sample time used in the experimental system. The consumer load is represented as a first order discrete transfer function (16)

$$G_l(z) = \frac{b}{z + a} \quad (16)$$

where $a, b \in \mathbb{R}$. The equations of the line voltage and damper load current of the SM are obtained using the expressions in (17) and (18), respectively.

$$V_L = \frac{48}{50} \times \sqrt{3} \quad (17)$$

$$I_{DL} = \frac{0.006419}{Z-1} \times \frac{-3}{2} \quad (18)$$

The structure of the SM is shown in Figure 4. The Generator transfer function block gives the output frequency. The input to this block is a unit step function (modelled as a constant block) used to emulate the per-unit HF model. The consumer load is simulated by subtracting the output of the consumer load transfer function from that of the generator. The input to the consumer load block is controlled by a switch with two inputs. The switch simulates turning ON and OFF of the consumer load by using a sine wave trigger to switch between Input 1 = 0 and Input 2 = 1. The ELC is simulated by subtracting the output of the PI controller from that of the generator with the feedback of the PI controller derived from the resultant output of the generator, consumer and PI controller. A gain block (c) is used to simulate the power rating of the dump loads in the experimental system. The line voltage and dump load currents are computed as products of the resultant frequency using expressions (17) and (18), respectively.

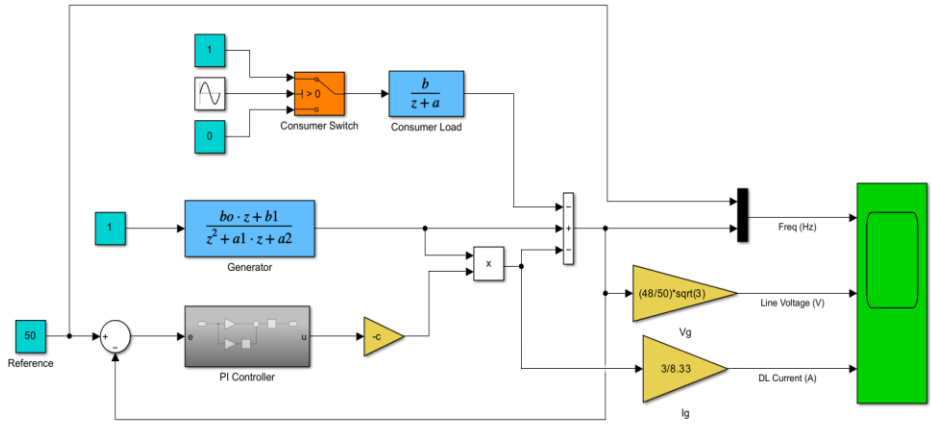

Figure 4: *Simplified Simulink model*

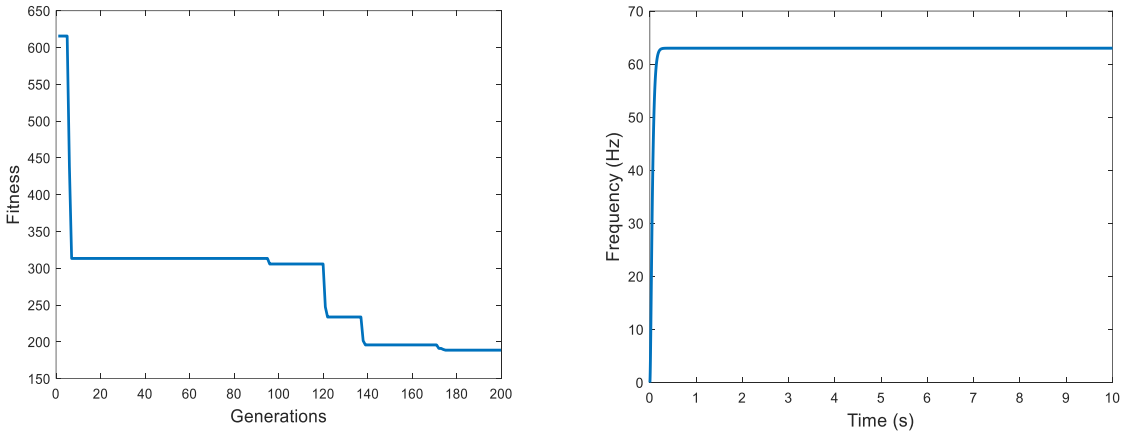

(a) (b)

Figure 5: *Simplified model parameter optimisation. (a) GA transfer function fitness, (b) Output frequency of generated transfer function.*

GA was used to optimise the gains of the SM's PI controller to achieve the best performance by minimising the integral of time absolute error (ITAE). The obtained PI parameter gains were then exported to the HF model and experimental system model for comparisons.

3. Results and Discussion

The simulation and experimental results of the GA simplified modelling and tuning of a PI-ELC to regulate the output frequency are presented in this section. In both cases, the GA is tuned using a population size of 10 for 200 generations.

3.1 Simulation results

Figure 5a shows the fitness function of the GA optimisation process used to identify the parameters of the SM transfer function, with the continuous time response of the identified system shown in Figure 5b. The SM was optimised for 200 generations to have an open loop response that is close to the open loop response of the experimental system. The open loop response of the experimental system is shown in Figure 6 where it can be observed that the experimental system has a fast rise time with a minimum and maximum frequency output (obtained after several experiments) of about 61 Hz and 65 Hz respectively. Therefore, the SM is tuned using a cost function with a step response of 63 Hz i.e., the average output frequency of the experimental system. The parameters of the continuous transfer function obtained via the GA optimisation are $k = 72700$ and $\omega_n = 34$ yielding the discrete transfer function (19).

$$G_{sm} = \frac{2.908z+2.318}{z^2-1.424z+0.5659} \quad (19)$$

The open-loop frequency outputs of the discrete SM and the HF model are also shown in Figure 6 where it can be observed that they converge to the average value (63 Hz) of the experimental system's open-loop output frequency. The main advantage of the simplified model is that it runs over 1000 times faster than the HF model (the HF model takes over 5 mins to run on a standard i5 Windows computer) thereby making the optimisation process feasible.

Figure 7 shows the result of the GA optimisation of the PI controller for the SM depicted in Figure 4. The resulting optimal values after searching for 200 generations were of 2.91 and 0.48 for k_p and k_i, respectively.

Figure 8 compares the closed-loop responses of applying the optimised PI gains to the SM and HF models simulated in MATLAB/Simulink environment. It can be observed that the output frequency for both the SM and HF models is maintained within ±1 Hz of the reference by the GA-tuned PI controller.

Figure 9(a) shows the overall current consumption of the HF model and simplified model, with the individual current drawn by each of the three damper loads, which depends upon the power channelled to each load by the controller. It is observed that the SM and HF model currents are fairly similar. Figure 9(b) illustrates the SM and HF model generator rms line voltage, exhibiting a minor voltage drop attributable to continuous load switching. In contrast, Figure 9(c) illustrates the regulated sine wave, wherein the SCR firing angle is deferred to modulate power distribution to the damper loads by the controller, therefore maintaining the desired generator speed and, consequently, the output frequency.

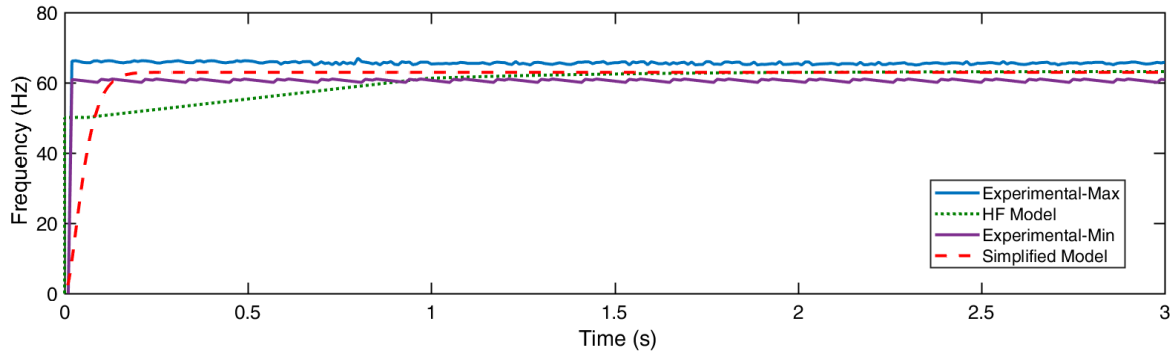

Figure 6: *Experimental generator, simplified and HF model open-loop frequency output*

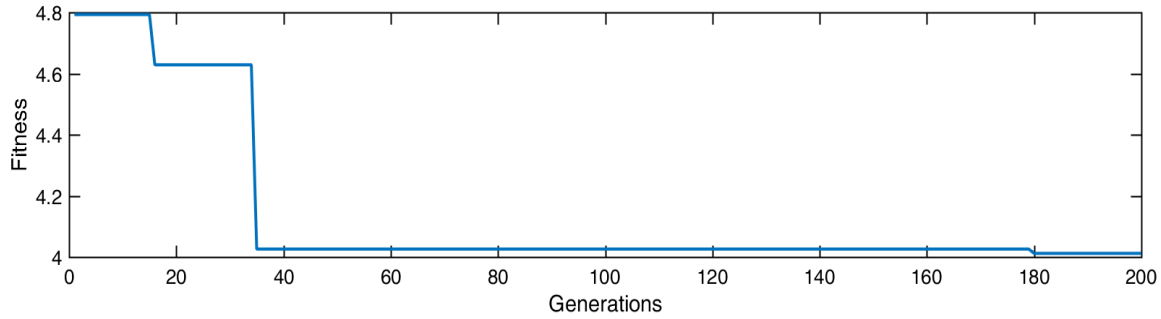

Figure 7: *SM PI controller GA fitness*

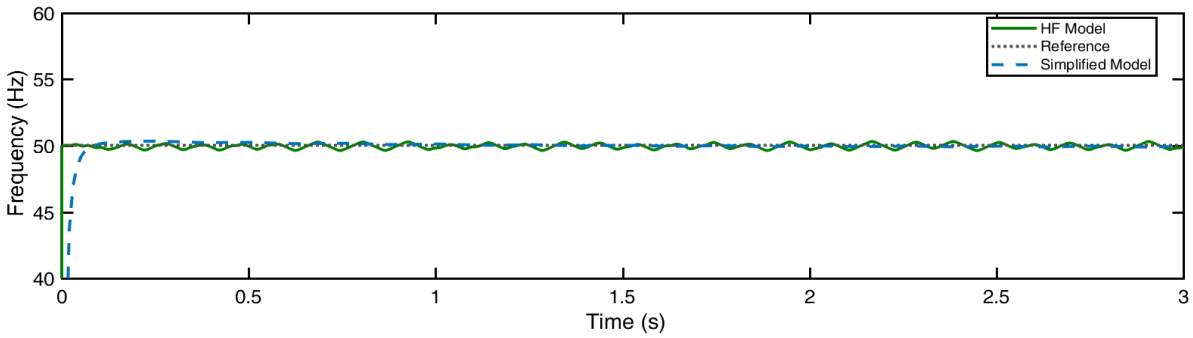

Figure 8: *Output frequency of the HF and SM*

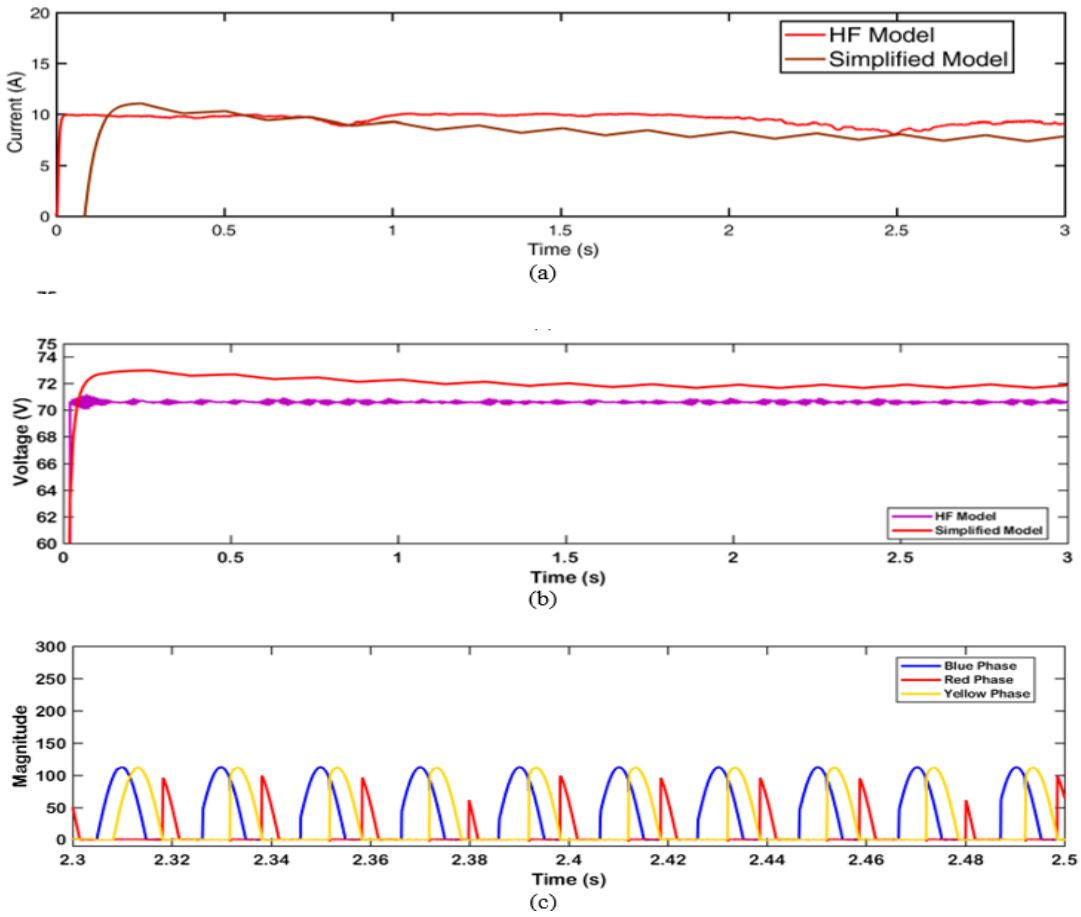

Figure 9: *SM and HF model outputs. (a) SM and HF model dump load current, (b) SM and HF model generator line voltage, (c) HF model chopped sine wave voltage across the SCRs*

3.2 Experimental results

Figure 10(a) shows the real time output responses of the experimental system using the optimised PI control parameters obtained via GA on the SM. It can be observed that after a transient noisy response, the experimental output frequency is maintained very close to the reference frequency within the acceptable tolerance of ± 1 Hz. Figure 10(b) and Figure 10(c) respectively, show the experimental line voltage and dump load currents, which are comparable to those obtained with the SM and HF models.

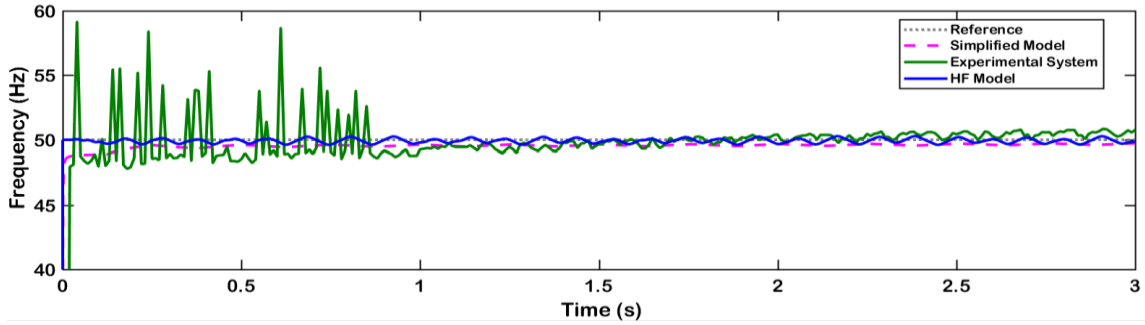

(a)

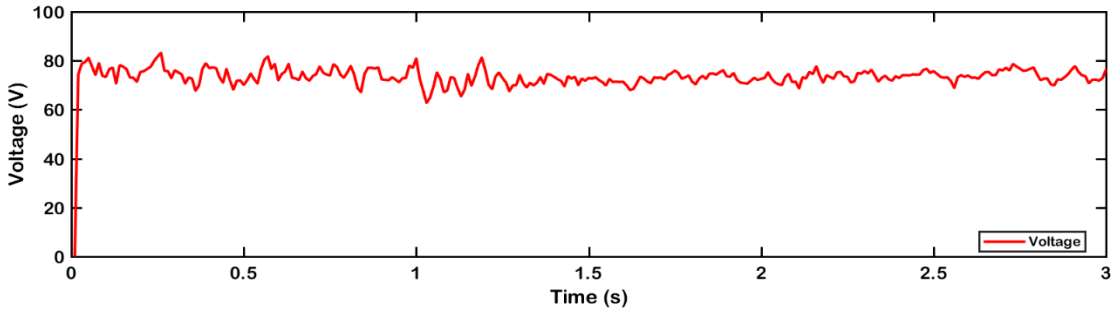

(b)

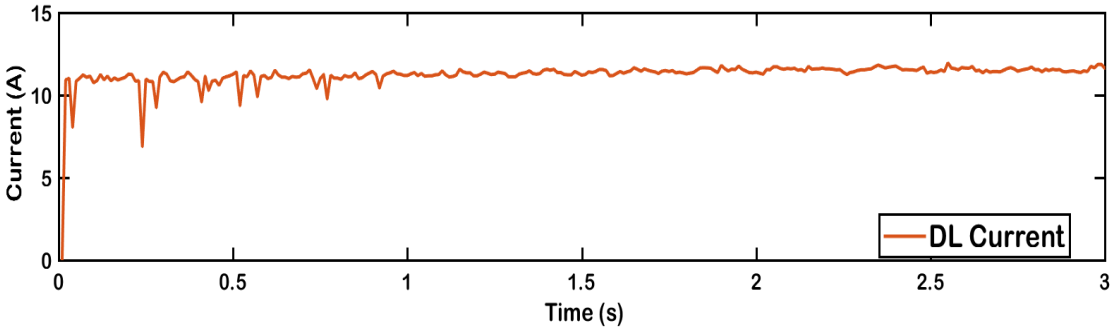

(c)

***Figure 10**: Experimental results. (a) Comparisons of experimental and simulation output frequency, (b) Generator line voltage, (c) Dump load current*

4. Conclusion

A relatively fast simplified model of an isolated generating system has been developed using a transfer function structure and GA optimisation to obtain the model parameters. The fairly accurate and fast simplified model enabled the use of GA optimisation to obtain the parameters of a PI based ELC designed using phase-cut modulation. The results of implementing the GA obtained PI parameters on a high-fidelity model by simulation and experimentally on the real-time system show that the proposed approach can be used to determine the PI controller parameters for ELCs of isolated power systems with satisfactory performance.

Acknowledgement

This research work was funded by the Nigerian Tertiary Education Fund (TETFund). Grant ID TETF/DR&D/CE/NRF/UNI/UDUS/STI/51/VOL1), 2019.

References

Abbas, I. A., & Mustafa, K. (2024). A review of adaptive tuning of PID-controller: Optimization techniques and applications. *Int. J. Nonlinear Anal. Appl*, *15*, 2008–6822. https://doi.org/10.22075/ijnaa.2023.21415.4024

Abdolrasol, M. G. M., Suhail Hussain, S. M., Ustun, T. S., Sarker, M. R., Hannan, M. A., Mohamed, R., Ali, J. A., Mekhilef, S., & Milad, A. (2021). Artificial neural networks-based optimization techniques: A review. In *Electronics (Switzerland) (Vol. 10, Issue 21). MDPI.* https://doi.org/10.3390/electronics10212689

Contreras, E., Herrero, J., Crochemore, L., Pechlivanidis, I., Photiadou, C., Aguilar, C., & Polo, M. J. (2020). Advances in the definition of needs and specifications for a climate service tool aimed at small hydropower plants' operation and management. *Energies*, *13*(7). https://doi.org/10.3390/en13071827

Haruna, A., Abdullahi, A. M., & Chaichaowarat, R. (2024). Variable Integral Adaptive Backstepping Hysteresis Admittance Compliant Control of Sensor less Single Joint Exoskeletons with Unknown Parameters. *IEEE Access*. https://doi.org/10.1109/ACCESS.2024.3506741

Haruna, A., Mohamed, Z., Efe, M., & Abdullahi, A. M. (2023). Switched step integral backstepping control for nonlinear motion systems with application to a laboratory helicopter. *ISA Transactions*, *141*, 470–481. https://doi.org/10.1016/J.ISATRA.2023.07.002

Haruna, A., Mohamed, Z., Efe, M., & Basri, M. A. M. (2020). Improved integral backstepping control of variable speed motion systems with application to a laboratory helicopter. *ISA Transactions*, *97*, 1–13. https://doi.org/10.1016/j.isatra.2019.07.016

Hino, T., & Lejeune, A. (2012). 6.15 - Pumped Storage Hydropower Developments. *Comprehensive Renewable Energy*, 405–434. https://doi.org/10.1016/B978-0-08-087872-0.00616-8

Katoch, S., Chauhan, S. S., & Kumar, V. (2021). A review on genetic algorithm: past, present, and future. *Multimedia Tools and Applications*, *80*(5), 8091–8126. https://doi.org/10.1007/s11042-020-10139-6

Khan, I. U., Javaid, N., Gamage, K. A. A., James Taylor, C., Baig, S., & Ma, X. (2020). Heuristic Algorithm Based Optimal Power Flow Model Incorporating Stochastic Renewable Energy Sources. *IEEE Access*, *8*, 148622–148643. https://doi.org/10.1109/ACCESS.2020.3015473

Kishore, T. S., Patro, E. R., Harish, V. S. K. V., & Haghighi, A. T. (2021). A comprehensive study on the recent progress and trends in development of small hydropower projects. In *Energies MDPI AG.* (Vol. 14, Issue 10). https://doi.org/10.3390/en14102882

Lambora, A., Gupta, K., & Chopra, K. (2019). Genetic Algorithm- A Literature Review. *Proceedings of the International Conference on Machine Learning, Big Data, Cloud and Parallel Computing: trends, perspectives and prospects: COMITCON-2019: 14th-16th February, 2019*. (2019). [IEEE].

Lü, X., Wu, Y., Lian, J., Zhang, Y., Chen, C., Wang, P., & Meng, L. (2020). Energy management of hybrid electric vehicles: A review of energy optimization of fuel cell hybrid power system based on genetic algorithm. In *Energy Conversion and Management Elsevier Ltd.* (Vol.205). https://doi.org/10.1016/j.enconman.2020.112474

Metwally, M. A., Ali, M. A., Kutb, S. A., & Bendary, F. M. (2019.). *A Genetic Algorithm for Optimum Design of PID Controller in Multi Area Load Frequency Control for Egyptian Electrical Grid*. www.ijert.org

Mirsaeidi, S., Devkota, S., Wang, X., Tzelepis, D., Abbas, G., Alshahir, A., & He, J. (2023). A Review on Optimization Objectives for Power System Operation Improvement Using FACTS Devices. In *Energies* (Vol. 16, Issue 1). MDPI. https://doi.org/10.3390/en16010161

Ortatepe, Z. (2023). Genetic Algorithm based PID Tuning Software Design and Implementation for a DC Motor Control System. *Gazi University Journal of Science Part A: Engineering and Innovation*, *10*(3), 286–300. https://doi.org/10.54287/gujsa.1342905

Papazoglou, G., & Biskas, P. (2023). Review and Comparison of Genetic Algorithm and Particle Swarm Optimization in the Optimal Power Flow Problem. In *Energies MDPI.* (Vol. 16, Issue 3). https://doi.org/10.3390/en16031152

Patil, R. S., Jadhav, S. P., & Patil, M. D. (2024). Review of Intelligent and Nature-Inspired Algorithms-Based Methods for Tuning PID Controllers in Industrial Applications. In *Journal of Robotics and Control (JRC)* (Vol. 5, Issue 2, pp. 336–358). https://doi.org/10.18196/jrc.v5i2.20850

Ruan, G., Zhong, H., Zhang, G., He, Y., Wang, X., & Pu, T. (2020). Review of Learning-Assisted Power System Optimization. https://doi.org/10.36227/techrxiv.12895337.v1

Sani, M. K., Haruna, A., Abdullahi, A. M., Muhammad, M., & Isa, A. I. (2024). Load Frequency Control for Standalone Power Generation with Open Source IoT Data Monitoring and Acquisition: A Tutorial. *www.njeabu.com.ng*

Shaheen, M. A. M., Hasanien, H. M., & Alkuhayli, A. (2021). A novel hybrid GWO-PSO optimization technique for optimal reactive power dispatch problem solution. *Ain Shams Engineering Journal*, *12*(1), 621–630. https://doi.org/10.1016/j.asej.2020.07.011

Shahgholian, G. (2020). An Overview of Hydroelectric Power Plant: Operation, Modeling, and Control. In *JREE* (Vol. 7, Issue 3).

Thirunavukkarasu, G. S., Seyedmahmoudian, M., Jamei, E., Horan, B., Mekhilef, S., & Stojcevski, A. (2022). Role of optimization techniques in microgrid energy management systems—A review. In *Energy Strategy Reviews* (Vol. 43). Elsevier Ltd. https://doi.org/10.1016/j.esr.2022.100899

Tyagi, S., Singh, B., & Das, S. (2022). ELD-OSG Control of a Battery-Based Electronic Load Controller for a Small Hydro Energy Conversion System. *IEEE Transactions on Industry Applications*, *58*(3), 3142–3152. https://doi.org/10.1109/TIA.2022.3149846

Yang, C., Sun, Y., Zou, Y., Zheng, F., Liu, S., Zhao, B., Wu, M., & Cui, H. (2023). Optimal Power Flow in Distribution Network: A Review on Problem Formulation and Optimization Methods. *In Energies (Vol. 16, Issue 16). Multidisciplinary Digital Publishing Institute (MDPI)*. https://doi.org/10.3390/en16165974

Yang, W. (2017). Hydropower plants and power systems Dynamic processes and control for stable and efficient operation. http://urn.kb.se/resolve?urn=urn:nbn:se:uu:diva-318470

Appendix

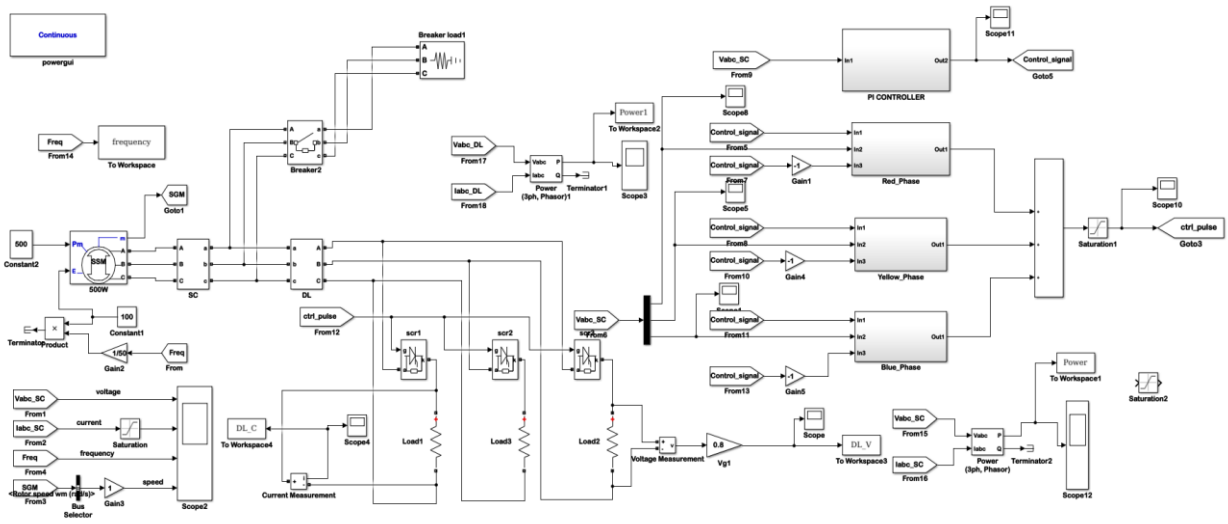

Figure A1: *Actual HF model PI controlled generating system Simulink block diagram*